Moving Coordinates Methods and applications to the oscillations of a falling slender body

Joey Y. Huang
Oak Ridge National Laboratory, USA

Abstract

We study the dynamical system of interaction between a rigid body and a viscid flow in two-dimensional space. The moving coordinates methods which can facilitate numerical simulations are introduced. This technique is applied to a moving ellipse and the simulations clearly demonstrate the oscillations of a falling slender body in a viscid flow. This phenomenon which has been noticed for over a century is obtained without any phenomenological model.

1 Introduction

The general problem of the motion of a rigid body in an inviscid flow has been studied since Kelvin and Kirchhoff in the 19th century (see Lamb [1]) while a general method to handle a rigid body moving in a viscid flow is still unavailable. However, the viscosity is quite important in many cases. The Kutta-Joukowski Theorem states that the force exerted on a body is normal to the direction of flow and is proportional to the circulation around the body. It means that there is no drag force and it contradicts our intuition and experiments. This is called d'Alembert's paradox (see Chorin & Marsden [2]) and it stems from the fact that the viscosity is ignored. A pitcher cannot pitch a curveball without the viscosity of the air. Coors Field (elevation 5,250 ft.) in Colorado is the famous "cemetery" of pitchers because of the low viscosity and density of the air. More importantly, no flow is really inviscid so it is essential to develop methods for the interaction between a solid body and a viscid flow. When the flow is very viscous, we can use Stokes' equations for the fluid and use boundary integral methods to handle the interaction (see Pozrikidis [3]). Kalthoff *et.al* [4] studied the

motion of a falling cylinder in a viscid flow when the Reynolds number is low. In Huang [5], a moving coordinate method is developed for a moving curveball in two-dimensional Navier-Stokes flow (it is a rotating cylinder moving in three-dimensional space). Even though it is applied in a special case only, this approach shows the possibility of handling the interaction without assuming the Reynolds number is high (without viscosity) or low (very viscous) .

The complicated motion of a piece of falling paper or a falling leaf in the air has been noticed for a long time. Maxwell [6] (1854) is the first scientist to comment on this phenomenon and he found the combination of gravity and lift results in a torque. Many physicists have tried to understand the behavior by experiments $[7-10]$. As yet, there's no satisfactory explanation for this complex behavior. Many phenomenological models have been introduced [11, 12, 15]. However, they either assume the flow is irrotational, or assume the drag force is proportional to the velocity, or combine the results from different kinds of flows to create models. A correct description for this question is still undetermined.

Belmonte *et.al* [16] presented a simple but illuminating laboratory experiment on flat strips dropped in a *quasi-2D* geometry. The experiment cell is a narrow fluid-filled glass aquarium. They found the patterns of the falling "paper" vary with length, weight and initial position. They also found the complicated shedding vortices of the flow behind a fluttering strip. There is similarity between their experiments and Huang's simulations of a moving curveball: they are both the interaction in *two-dimensional* space and some vortices are created by the motion of the objects.

In this paper, we set up the dynamical system of a rigid body moving in a viscid flow in two-dimensional space by Newton's second law and Navier-Stokes equations. We use *complex variables* $\mathbf{z} = x + iy$ to represent the position, velocity and force which are proved efficient in two-dimensional flow. The idea of moving coordinates methods is introduced and we explain how the dynamics of a moving curveball are rewritten in coordinates moving with the ball to facilitate numerical simulations. We apply this technique to the motion of an ellipse in a viscid flow. When a slender ellipse is dropped, oscillations of this object and the vortices of the flow are found that are quite similar to the experiments of Belmonte *et.al.* [16].

2 The dynamical system

Assume the boundary of a rigid body B is

$$\boldsymbol{\gamma}(\theta)\,, \text{ with periodic condition } \boldsymbol{\gamma}(\theta + 2\pi) = \boldsymbol{\gamma}(\theta)$$

The body is moving in a two-dimensional flow with the position $\mathbf{q}(t)$ of mass center and the angular position $\phi(t)$. The boundary of this object *in space* is

$$\mathbf{q}(t)+\boldsymbol{\gamma}(\theta)e^{i\phi(t)}\equiv\mathbf{q}(t)+\check{\boldsymbol{\gamma}}(\theta,t)$$

The normal direction of the boundary in space is

$$\mathbf{n}(\theta,t)=-i\frac{\boldsymbol{\gamma}_\theta(\theta)}{|\boldsymbol{\gamma}_\theta(\theta)|}e^{i\phi(t)},\ \boldsymbol{\gamma}_\theta=\frac{d\boldsymbol{\gamma}}{d\theta}$$

and the infinitesimal length ds of the boundary is

$$ds=|\boldsymbol{\gamma}_\theta(\theta)|\,d\theta$$

The dynamical system of the interaction is the combination of PDEs and ODEs:

$$\begin{aligned}
\mathbf{u}_t+(\mathbf{u}\cdot\nabla)\mathbf{u} &= -\nabla\left(\frac{p}{\rho}\right)+\nu\Delta\mathbf{u} && (1)\\
\nabla\cdot\mathbf{u} &= 0 && (2)\\
\mathbf{q}_t &= \mathbf{v}\\
M\mathbf{v}_t &= -\int_{\partial B}(p\mathbf{n}-\boldsymbol{\sigma}\cdot\mathbf{n})\,ds+M\mathbf{g}+\mathbf{F} && (3)\\
\phi_t &= \omega\\
I\omega_t &= -\int_{\partial B}\check{\boldsymbol{\gamma}}\times(p\mathbf{n}-\boldsymbol{\sigma}\cdot\mathbf{n})\,ds+L && (4)\\
\boldsymbol{\sigma} &\equiv \rho\nu\left(\nabla\mathbf{u}+(\nabla\mathbf{u})^T\right)
\end{aligned}$$

Eqns (1) , (2) are the well-known Navier-Stokes equations for the fluid where $\mathbf{u}$, p, ρ, ν are the velocity, pressure, constant density and viscosity of the fluid. Eqns (3) , (4) are the balances of momentum and angular momentum of the object where $\mathbf{v}$, ω, M, I are the velocity, rotational speed, mass and inertia tensor of the object. $\mathbf{F}(t)$ and $L(t)$ are the force and torque from other sources. The outer product "$\times$" is defined by

$$\mathbf{a}\times\mathbf{b}\equiv a_1b_2-a_2b_1$$

The no-slip conditions of the viscous fluid on the boundary and in infinity are

$$\begin{aligned}
\mathbf{u}|_{\partial B} &= \mathbf{v}+i\omega\boldsymbol{\gamma}e^{i\phi}\\
\mathbf{u}|_{\infty} &= 0
\end{aligned}$$

The trajectory $\mathbf{q}(t)$ and angular position $\phi(t)$ of the object are determined by this complex dynamical system and so is the velocity $\mathbf{u}(\mathbf{z},t)$ of the fluid everywhere. Note that the dynamical system is not a phenomenological model. It is based on Newton's second law and Navier-Stokes equations which are derived from conservation of the fluid's mass and momentum.

3 Moving coordinates methods

The best way to study the fluid around a moving rigid body is to use the coordinates moving with the object because the boundary is fixed in the coordinate system. This approach has been widely used for the fluid around a moving circular or elliptical cylinder when the velocity and angular speed of the object are given. However, the difficulty of using this approach for the interacting system in Section 2 is that the motion of the object is unknown – it is determined by the system itself. Kalthoff *et.al.* [4] used fixed Cartesian coordinates for the fluid when studying a free falling cylinder in a viscid flow. Because the mesh points conflict with the moving boundary, they use an analytical expansion based on low Reynolds number flow to evaluate the force exerted on the cylinder and their approach is thus limited. When the boundary of the object is a circle,

$$\boldsymbol{\gamma}(\theta) = Re^{i\theta} \tag{5}$$

Huang [5] used this coordinates transformation even though the trajectory $\mathbf{q}(t)$ is unknown:

$$\begin{cases} \check{\mathbf{z}} = \mathbf{z} - \mathbf{q}(t) \\ \check{t} = t \end{cases} \tag{6}$$

The boundary is *fixed* in coordinates $\left(\check{\mathbf{z}}, \check{t}\right)$ and the interacting system was successfully rewritten in the free moving polar coordinates $\left(s, \theta, \check{t}\right)$ where

$$\check{\mathbf{z}} = Re^{s+i\theta} \tag{7}$$

A moving curveball is thus achieved and so is the behavior of the fluid around the object. Figure 1 illustrates the idea of this moving coordinates technique and how the conflict between mesh points and moving boundary is eliminated.

In this paper, we apply the moving coordinates methods to another special case: an elliptic object. The boundary $\boldsymbol{\gamma}$ is

$$\boldsymbol{\gamma}(\theta) = R\cosh(\varepsilon + i\theta) \tag{8}$$

When ε is small, it is a slender ellipse which is similar to the strip in the experiments of Belmonte *et.al.* [16].

In this case, the coordinates transformation (6) is not sufficient to eliminate the conflict between mesh points and the object's boundary because $|\boldsymbol{\gamma}(\theta)|$ is not a constant. We need this coordinates transformation:

$$\begin{cases} \check{\mathbf{z}} = e^{-i\phi(t)}\left(\mathbf{z} - \mathbf{q}(t)\right) \\ \check{t} = t \end{cases} \tag{9}$$

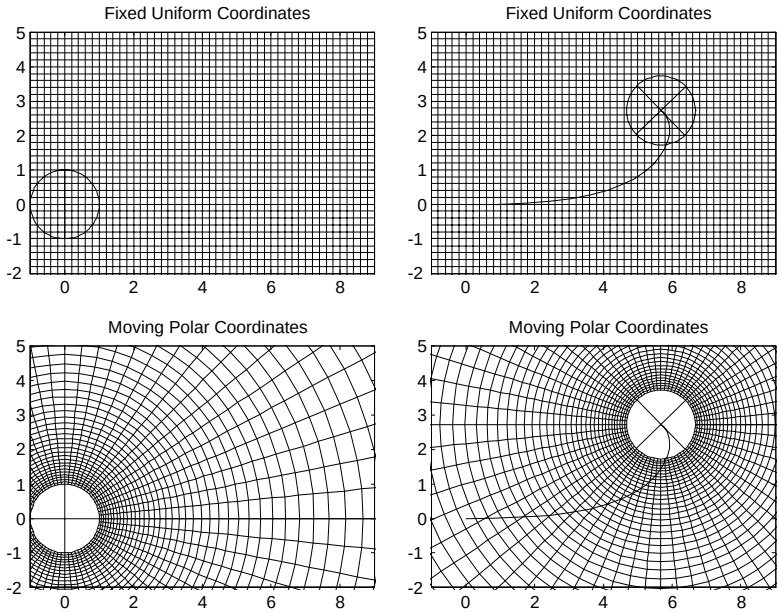

Figure 1: The advantage of moving coordinates for the interacting system.

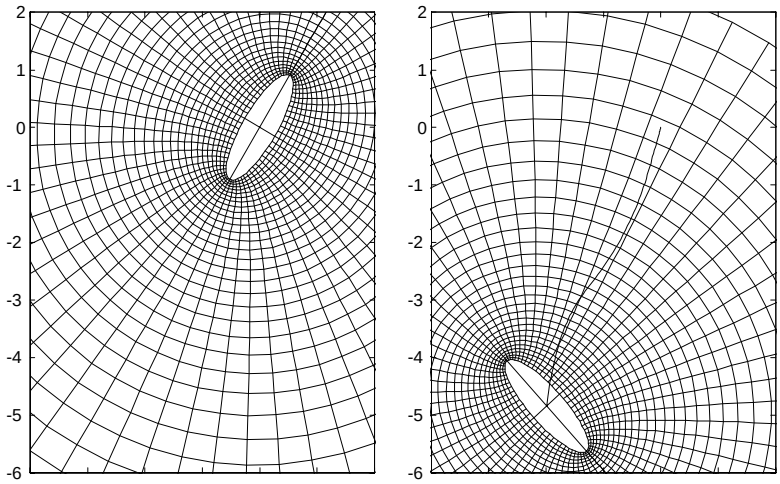

Figure 2: The moving coordinates for the ellipse.

Now the coordinates are not just moving with the object but also rotating. The boundary is thus fixed in $\left(\check{\mathbf{z}}, \check{t}\right)$ and we introduce the elliptic coordinates to fit the boundary:

$$\check{\mathbf{z}} = R\cosh\left(\varepsilon + s + i\theta\right) \tag{10}$$

Figure 2 demonstrates the moving elliptic coordinates (10).

The stream-function vorticity formulations in the moving coordinates $\left(s,\theta,\check{t}\right)$ (we use t instead of $\check{t}$ in the final equations):

$$\begin{aligned} W\xi_t + \psi_s\xi_\theta - \psi_\theta\xi_s &= \nu\left(\xi_{ss}+\xi_{\theta\theta}\right) && (11)\\ W &= R^2\left(\sinh^2\left(\varepsilon+s\right)+\sin^2\theta\right) \\ \psi_{ss}+\psi_{\theta\theta} &= W\left(\xi-2\omega\right) && (12)\end{aligned}$$

Here ψ is the stream function in the moving coordinates while ξ still represents the vorticity observed in fixed coordinates (thus the extra term -2ω in Eqn (12) .).

The ODEs for the ellipse in the moving coordinates are

$$\begin{aligned} \acute{M}\left(\mathbf{v}_t-\mathbf{g}\right) &= \pi i R\rho\nu e^{i\phi}\left(e^{\varepsilon}\left(\hat{\xi}^{-1}-\hat{\xi}_s^{-1}\right)-e^{-\varepsilon}\left(\hat{\xi}^{1}+\hat{\xi}_s^{1}\right)\right)|_{\partial B} && (13)\\ &\quad +\mathbf{F} \\ I\omega_t &= \pi R^2\rho\nu\left(\hat{\xi}^0\sinh\left(2\varepsilon\right)-\frac{\hat{\xi}_s^2+\hat{\xi}_s^{-2}}{4}\right)|_{\partial B} && (14)\\ &\quad -2\pi R^2\rho\nu\sinh\left(2\varepsilon\right)\omega+L \\ \acute{M} &\equiv M-\frac{\pi R^2\rho}{2}\sinh\left(2\varepsilon\right)\end{aligned}$$

$\hat{\xi}^n$ (or $\hat{\xi}_s^n$) is the Fourier transform of ξ (or ξ_s).

Eqns(11), (12), (13) and (14) represent the dynamics in the moving coordinates which are similar to what Huang has derived for a moving curveball in [5]. Furthermore, when $\tilde{R}\equiv Re^{\varepsilon}/2$ is fixed and $\varepsilon\to\infty$, the boundary (8) becomes a circle $\tilde{R}e^{i\theta}$ and we can verify that the equations we get here are equivalent to the equations for a moving curveball.

4 Numerical simulations

We apply this dynamical system to simulate a free falling slender ellipse. It is similar to a falling flat strip in a narrow fluid-filled glass aquarium or a falling slender elliptic cylinder in three-dimensional space which is similar to a piece of paper. When $t<0$, the extra force is $\mathbf{F}=-\acute{M}\mathbf{g}$ to balance the gravity (see Eqn (13)). The ellipse is released when $t=0$ and $\mathbf{F}=\mathbf{0}$ when $t>0$. After the system is nondimensionalized, R, ν, $\rho=1$ and the intrinsic parameters are ε, M, I and $\mathbf{g}$. If the ellipse has uniform density, the density d determines both M and I. We choose $\varepsilon=0.3$, $d=2$, $g=1000$ and the initial angular position $\phi_0=\pi/3$ in the simulations. Figures 3 and 4 indicate the trajectory, the oscillations of the falling slender body and vorticity contour. The positions of the falling object are "shot" with the uniform time interval $\Delta t=0.02$. We can see the oscillations create the vortices around the object and how the vortices cause the oscillations which coincide with the experiments of Belmonte *et.al.* [16].

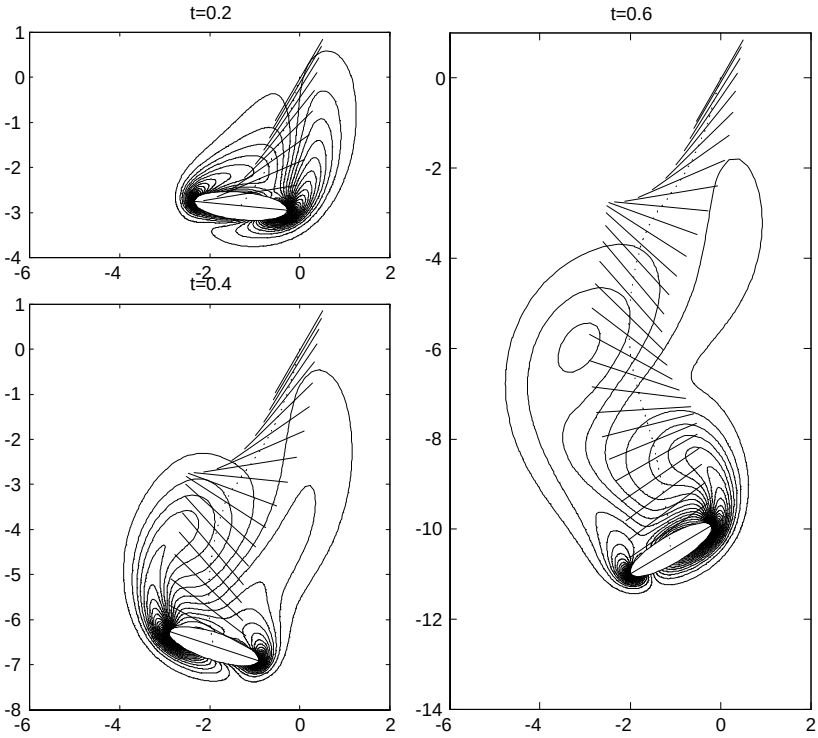

Figure 3

Figure 5 is a close-up shot of the vorticity contour when $t = 0.7$. The animated movies of this simulations (streamline plot and vorticity in colormap) are available in the web site {http://www.csm.ornl.gov/~huang/fall.htm}.

5 Conclusions

Even though it is in two-dimensional space only, we have successfully described the motion of a falling slender body in a viscid flow without any phenomenological model. The extension of this moving coordinates approach to three-dimensional space is possible, though it could be quite complicated: we cannot use complex variables in three dimensional space; the vorticity is a vector instead of a scalar. The first step would be motion of a sphere in a three-dimensional flow instead of a piece of falling paper which is definitely more complicated. On the other hand, we have applied the moving boundary methods in two special cases. It is possible that we can derive general formulas for the motion of a rigid body in two-dimensional viscid flow.

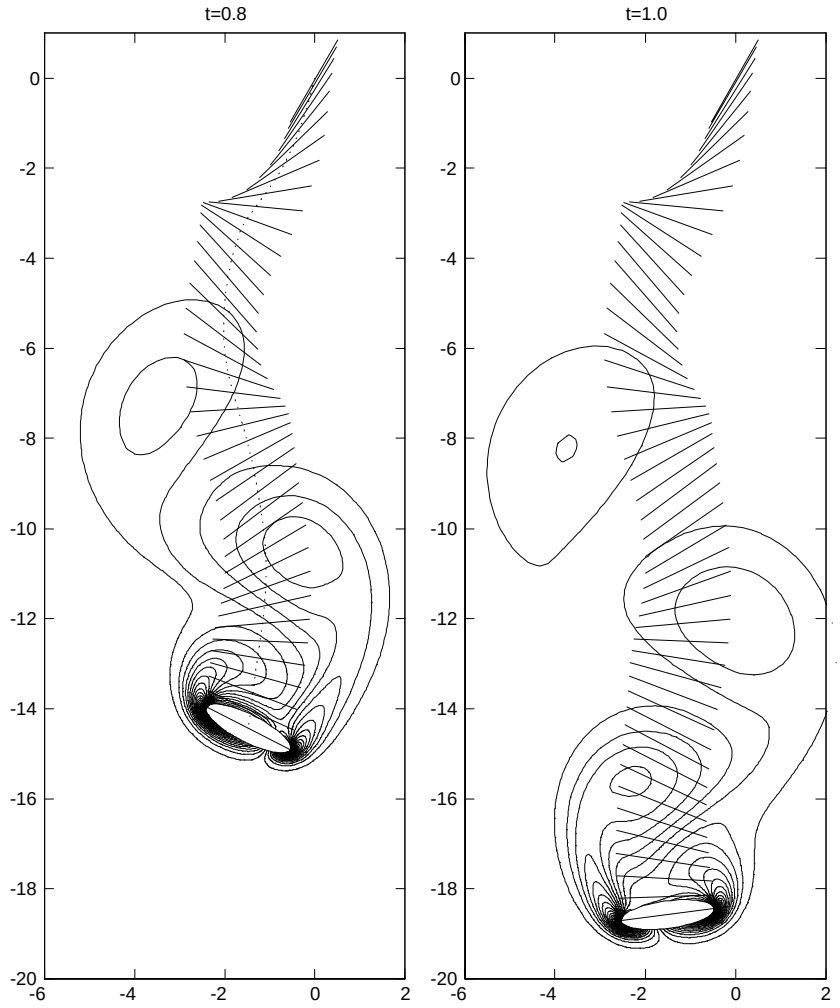

Figure 4

Acknowledgment

The author would like to thank Charles H. Romine and Eduardo D'Azevedo for useful suggestions for this paper. This research was supported in part by the Applied Mathematical Sciences Research Program of the Division of Mathematical, Information, and Computational Sciences, U.S. Department of Energy under contract DEAC0500OR22725 with UT-Battelle, LLC.

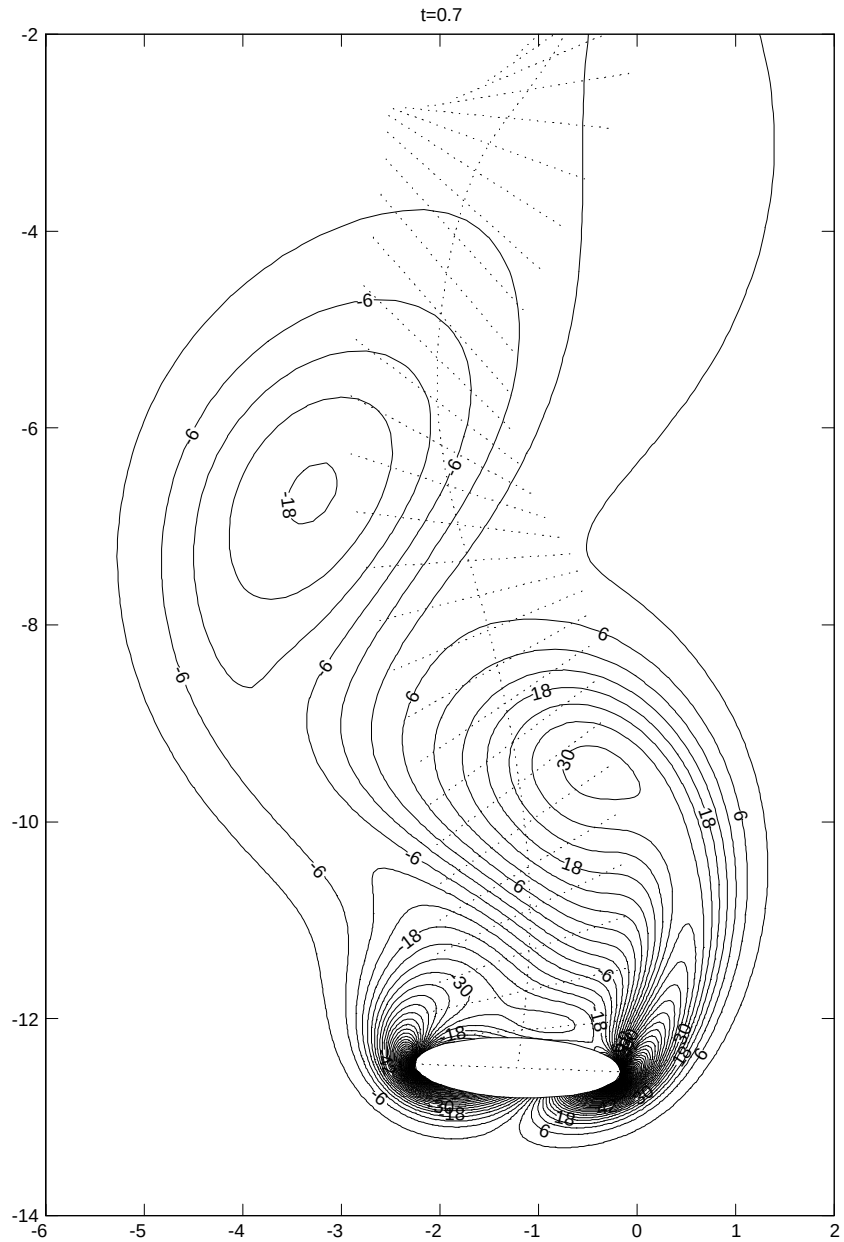

Figure 5

References

[1] Lamb, H. *Hydrodynamics,* Dover, New York, 1945.

[2] Chorin, A.J. & Marsden, J.E. *A Mathematical Introduction to Fluid Mechanics,* Springer-Verlad, 1992.

[3] Pozrikidis, C. *Boundary Integral and Singularity Methods for Linearized Viscous Flow,* Cambridge University Press, Cambridge, 1992.

[4] Kalthoff, W., Schwarzer, S. & Hermann, H.J. Algorithm for the simulation of particle suspensions with inertia effects. *Phys. Rev. E,* **56**, pp. 2234-2242, 1997.

[5] Huang, J.Y. Aerodynamics of a curveball in 2D Navier-Stokes flow (submitted to *Phys. Fluids*).

[6] Maxwell, J.C. On a particular case of the descent of a heavy body in a resisting medium. *The Scientific Papers of James Clerk Maxwell,* pp. 115-118, 1890.

[7] Willmarth, W., Hawk, N. & Harvey, R. Steady and unsteady motions and wakes of freely falling disks. *Phys. Fluids,* **7**, pp. 197-208, 1964.

[8] Stewart, R.E. & List, R. Gyrational motion of disks during free-fall. *Phys. Fluids,* **26**, pp. 920-927, 1983.

[9] Trankle, E. & Riikonen, M. Elliptical halos, Bottlinger's rings, and the ice-plate snow-star transition. *Appl. Opt.,* **35**, pp. 4871-4878, 1996.

[10] Field, S., Klaus, M., Moore, M. & Nori, F. Chaotic dynamics of falling disks. *Nature,* **388**, pp. 252-524, 1997.

[11] Aref, H. & Jones, S.W. Chaotic motion of a solid through ideal fluid. *Phys. Fluids A,* **5**, pp. 3026-3028, 1993.

[12] Tanabe, Y. & Kaneko, K. Behavior of a falling paper. *Phys. Rev. Lett.,* **73**, pp. 1372-1375, 1994.

[13] Mahadevan, L., Aref, H. & Jones, S.W. Comment on "Behavior of a falling paper". *Phys. Rev. Lett.,* **75**, pp. 1420, 1995.

[14] Tanabe, Y. & Kaneko, K. *Phys. Rev. Lett.,* **75**, pp. 1421, 1995.

[15] Mahadevan, L. Tumbling of a falling card. *C. R. Acad. Sci.,* **323**, pp. 729-736, 1996.

[16] Belmonte, A., Eisenberg, H. & Moses, E. From flutter to tumble: Inertial drag and Froude similarity in falling paper. *Phys. Rev. Lett.,* **81**, pp. 345-348, 1998.

[17] Belmonte, A. and Moses, E. Flutter and tumble in fluids. *Phys. World,* **12**, pp. 21-25, 1999.